JOURNAL OF COMPARATIVE NEUROLOGY 229:432-450 (1984)

The Central Projections of Intracellularly Labeled Auditory Nerve Fibers in Cats

D.M. FEKETE, E.M. ROUILLER, M.C. LIBERMAN, AND D.K. RYUGO
Departments of Anatomy (D.M.F., D.K.R.) and Physiology (M.C.L.), Harvard Medical School, Boston, Massachusetts 02115, and Eaton-Peabody Laboratory of Auditory Physiology (D.M.F., E.M.R., M.C.L., D.K.R.), Massachusetts Eye and Ear Infirmary, Boston, Massachusetts 02114

ABSTRACT

The central projections of physiologically characterized auditory nerve fibers were studied in the cochlear nuclei of adult cats after intracellular staining with horseradish peroxidase (HRP). This technique consistently labels only the type I spiral ganglion neurons which contact inner hair cells in the cochlea (Liberman and Oliver, '84). The central axon of each type I neuron bifurcates in the cochlear nucleus to form an ascending branch and a descending branch. The characteristic frequency (CF) of a fiber corresponds to the dorsoventral position of these major branches and their collateral ramifications within the nucleus. Fibers of low CFs are distributed ventrally, and fibers of increasing CF are distributed progressively more dorsally. In some cases, the collateral branches deviate from this tonotopic arrangement, particularly in (1) the octopus cell region of the posteroventral cochlear nucleus, (2) the zone of bifurcations of the auditory nerve fibers, and (3) the anterior, dorsal, and lateral margins of the ventral cochlear nucleus. Spontaneous discharge rate (SR) is related to the complexity of the axon arbor, especially along the ascending branch. Fibers of low and medium SR exhibit more axonal branch points and longer collateral lengths than do those with high SR. Six of 37 labeled fibers fail to innervate the dorsal cochlear nucleus, a feature apparently unrelated to CF or SR.

Key words: auditory nerve, cochlear nucleus, hearing, primary afferents

In the mammalian auditory system, transduction of sound stimuli by acoustic receptors in the cochlea results in discharges in the primary sensory neurons of the spiral ganglion. The central axons of the spiral ganglion cells bundle together to form the auditory nerve and project to the ipsilateral cochlear nucleus. As the initial synaptic station in the central auditory pathway, the cochlear nucleus represents the first opportunity to process the incoming discharges of the auditory nerve. The cells of the cochlear nucleus systematically vary in their afferent innervation (Osen, '70; Brawer and Morest, '75; Cant and Morest, '78; Lorente de Nó, '81), cellular morphology (Osen, '69; Brawer et al., '74; Mugnaini et al., '80), central projections (Harrison and Feldman, '70; Ryugo et al., '81; Cant, '82; Tolbert et al., '82; Warr, '82; Adams, '83;), and physiological responses to sound stimuli (Pfeiffer, '66; Godfrey et al., '75a,b; Young and Brownell, '76). The processing of auditory information by the different classes of cochlear nucleus neurons will depend in large part on the anatomical organization of their primary input. Knowledge of this organization is of fundamental importance in formulating models for the central processing of auditory information (Kiang, '75; Tsuchitani, '78). Such models will necessarily be different if, for example, all auditory nerve fibers have a similar projection pattern in the cochlear nucleus (as was implied by Lorente de Nó, '33), or if instead, specific groups of fibers selectively innervate different cell types (or parts of cells).

Accepted June 27, 1984.

Address reprint requests to Dr. D.K. Ryugo, Department of Anatomy, Harvard Medical School, 25 Shattuck Street, Boston, MA 02115.

D.M. Fekete's present address is MRC Cell Biophysics Unit, 26-29 Drury Lane, London WC2B 5RL, England.

E.M. Rouiller's present address is Department of Physiology, School of Medicine, Rue de Bugnon 7, 1011 Lausanne, Switzerland.

Much of our present knowledge of the central terminations of primary auditory neurons has been obtained from studies using the Golgi technique (Held, 1893; Vincenzi, '01; Ramón y Cajal, '09; Lorente de Nó, '33, '81; Morest, '68; Feldman and Harrison, '69; Brawer and Morest, '75). This method has been very useful in elucidating the structure of individual primary neurons but works best in neonatal and young animals. Recently, it was demonstrated that significant changes occur in the terminal morphology of auditory nerve fibers as cats mature (Ryugo and Fekete, '82). Thus, Golgi descriptions may not be representative of auditory nerve fibers in mature animals.

The present study focuses on the central projections of type I spiral ganglion neurons in the mature cat. Type I cells comprise 90–95% of the spiral ganglion population and have cell bodies that are large, generally bipolar, and myelinated. Their peripheral processes contact inner hair cells (Spoendlin, '69; Kiang et al., '82). The thick, myelinated central axons of these neurons have proven to be readily accessible to both extra- and intracellular recordings (Kiang et al., '65; Sachs and Abbas, '74; Liberman, '78, '82a,b; Kim and Molnar, '79; Sachs and Young, '79; Young and Sachs, '79; Evans and Palmer, '80; Schalk and Sachs, '80). Nothing is known about the response properties of type II neurons which contact outer hair cells (Liberman, '82a).

Two of the most important functional properties of type I neurons are their tuning curves and spontaneous discharge rates (SRs). Once these properties have been determined, many additional aspects of a neuron's physiology and morphology can be predicted. The characteristic frequency (CF) of a neuron, the tone frequency to which it is maximally sensitive, provides a direct measure of the longitudinal position of its peripheral terminal along the cochlear spiral (Liberman, '82b). SR is the average discharge rate in the absence of controlled acoustic stimulation and is related to the caliber and position of the terminal segment contacting the inner hair cell (Liberman, 82a). Since it has been shown that type I fibers can be separated into different groups on the basis of their physiological responses (e.g., Liberman, '78, '82a,b; Evans and Palmer, '80), we have begun investigating whether such groupings correlate with anatomical distinctions in central morphology or connectivity.

The present report provides a general description of the axonal projections of individual spiral ganglion neurons that have been electrophysiologically characterized and stained by intracellular recording techniques. Certain morphological features (e.g., spatial distribution, fiber lengths, and number of branch points) have been quantified and are shown to be related to the physiological response properties of CF or SR.

MATERIALS AND METHODS

Physiological recordings

A total of 18 cats, each weighing between 1.75 and 3.4 kg, were used for intra-axonal recordings from auditory nerve fibers. In four cats, recordings were made from the nerve on both sides. The anesthetic and surgical preparation, the means of presenting acoustic stimuli, and the techniques for recording and processing single-unit activity have been previously described (Kiang et al., '65; Liberman, '78). Techniques for intracellular recording and iontophoresis of horseradish peroxidase (HRP) were identical to those described elsewhere (Liberman, '82a,b). For each unit, a tuning curve and a 15- or 30-second sample of spontaneous activity (SR) were obtained before and after the injection of HRP. The DC resting potential was monitored throughout (Fig. 1). Continuity of the intracellular DC potential and close similarities in the pre- and postinjection response properties (shapes of tuning curves, CF, and SR) indicated that the electrode maintained contract with the same neuron during the recording and injection period.

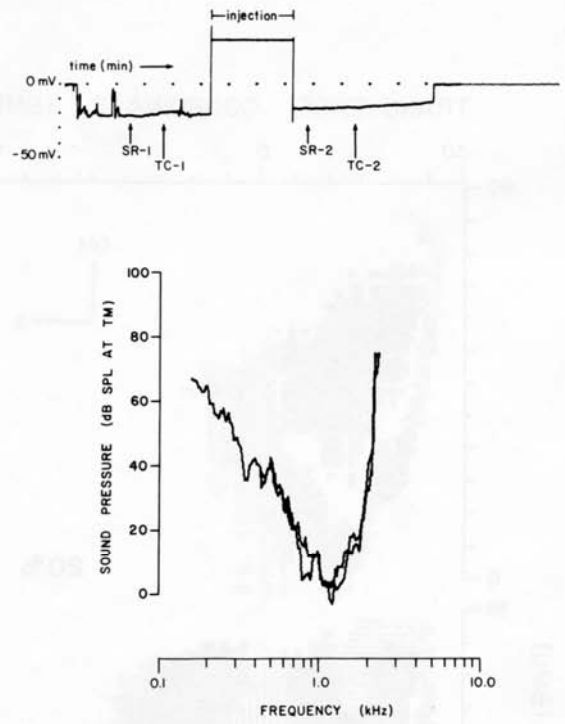

Fig. 1. DC potential (top) and tuning curves (bottom) measured from a single auditory nerve fiber intracellularly injected with HRP. Iontophoretic injection of HRP was accomplished by passing a positive current of 4.5 namp for 3 minutes through the micropipette. During this time, the resting potential was visually monitored on the oscilloscope. The vertical arrows indicate when recordings of spontaneous rate (SR) and threshold tuning curves (TC) were initiated. SR-1 and SR-2 were 85.9 and 81.9 spikes/second, respectively. In the bottom plot, TC-1 (incomplete below 0.4 kHz) and TC-2 have been superimposed. Characteristic frequencies (CFs) determined before and after the injection of HRP were 1.20 and 1.28 kHz, respectively. Abbreviations: dB, decibel; min, minutes; mV, millivolt; kHz, kiloHertz; SPL, sound pressure level; TM, tympanic membrane.

Histological procedures

Each animal was perfused 20–24 hours following the last injection, and tissue was postfixed as described previously (Ryugo and Fekete, '82). For the 22 auditory nerves and cochlear nuclei in this study, the cochleas were processed in ten cases; the analysis of data from these cochleas has been reported elsewhere (Liberman, '82a,b).

The auditory nerve, cochlear nucleus, and adjacent brain stem were isolated in a single tissue block. Each block was photographed to aid in subsequent three-dimensional reconstructions of the tissue, embedded in a gelatin-albumin mixture (Frank et al., '80), then sectioned at 40–100 μm on a Vibratome. The plane of section was nearly parallel to the lateral surface of the cochlear nucleus, forming an angle of 40° with the standard sagittal plane (fig. 2). This "modified sagittal" plane minimizes the number of histological sections required to span the nucleus and the num-

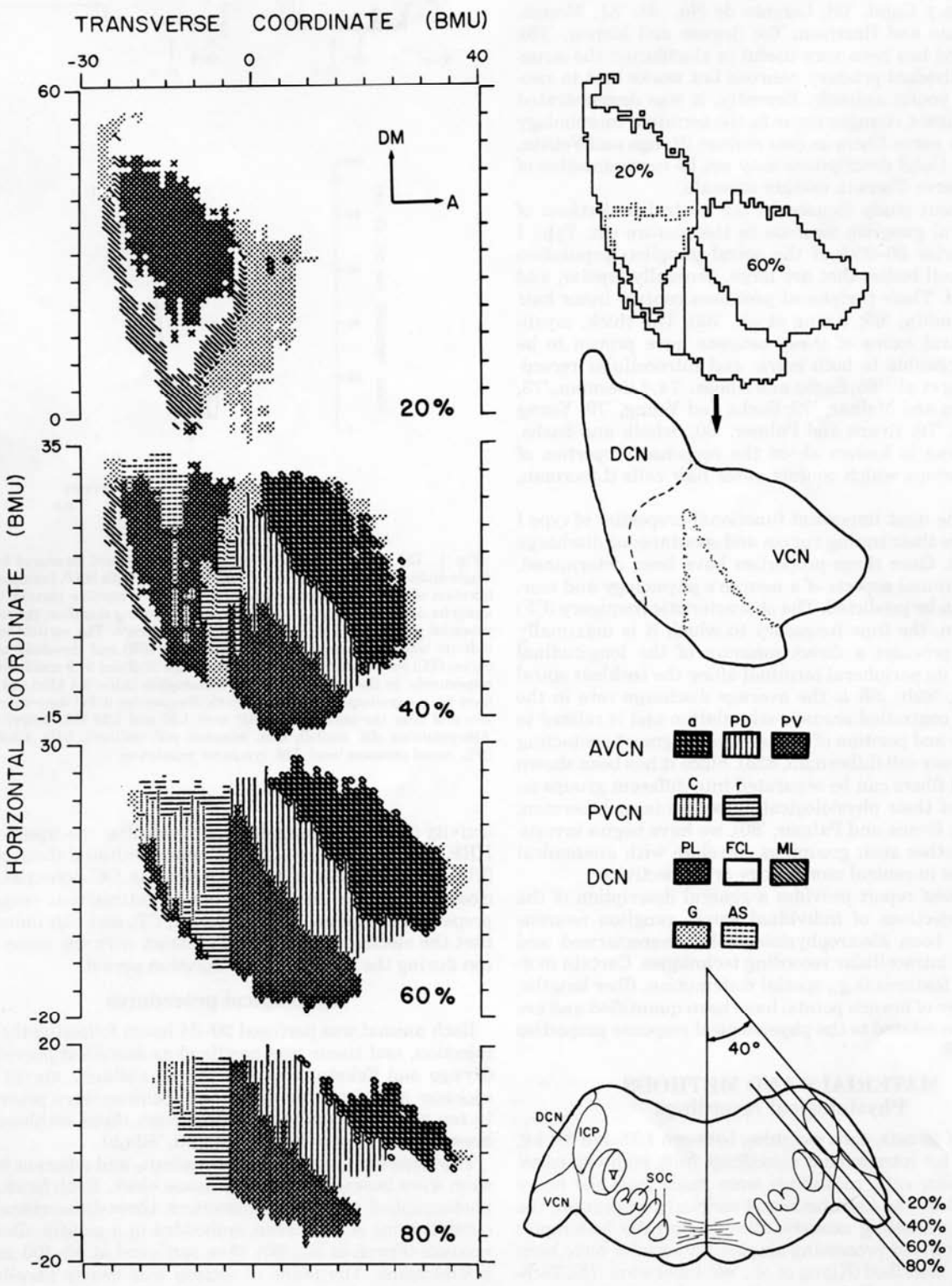
TRANSVERSE COORDINATE (BMU)
-30
0
40
60
0
DM
A
20%
35
-15
40%
30
-20
60%
20
-20
80%
HORIZONTAL COORDINATE (BMU)
20%
60%
DCN
VCN
AVCN
α
PD
PV
PVCN
C
r
DCN
PL
FCL
ML
G
AS
40°
DCN
ICP
V
SOC
VCN
20%
40%
60%
80%

Figure 2

ber of sections containing a single auditory nerve fiber. Thus, visual distortion resulting from two-dimensional reconstructions of three-dimensional fibers are minimized.

Free-floating tissue sections were serially collected, rinsed several times in 0.1M tris buffer, pH = 7.6, and incubated for 1 hour in 0.5% $CoCl_2$ and 1% dimethylsulfoxide (DMSO) in tris buffer. After washing in tris buffer (2 × 5 minutes) and 0.1 M phosphate buffer, pH = 7.3 (2 × 5 minutes) the sections were incubated for 1 hour with 0.05% 3,3′-diaminobenzidine (DAB); Sigma grade II TetraHCl), 1% DMSO, and 0.01% H_2O_2, followed by extensive rinsing in phosphate buffer (minimum 4 × 5 minutes). Fifteen cochlear nuclei were prepared for light microscopy by mounting sections onto gelatin-subbed slides, air-drying overnight, counterstaining with cresyl violet, and coverslipping with Permount.

Seven cochlear nuclei were processed for electron microscopy, and in these cases, DMSO was omitted from the HRP reaction procedure. Following the histochemical reaction, free-floating tissue sections were immersed in 1% osmium tetroxide in 0.12 M phosphate buffer (15 minutes), stained en bloc with 2% uranyl acetate (1 hour) or 1% uranyl acetate (overnight) dehydrated through graded methanol solutions, infiltrated with Epon, and embedded between two transparent sheets of Aclar (Allied Chem. Co.) Once the Epon polymerized, each tissue section (along with a surrounding margin of Epon) was cut out and taped to a microscope slide for light-microscopic analysis, while still sandwiched between the Aclar sheets.

Selected areas of interest were prepared for ultrastructural analysis. Before thin sections were cut, light-microscopic drawings (1,250×) of the labeled structure, complete with details on surrounding landmarks (including cells, blood vessels, and tissue borders), were traced at successive 4-μm focal planes within the 40-μm section so that orientation could be maintained during examination with the electron microscope. The labeled structure was then isolated within a smaller Epon piece using razor cuts, the Aclar was peeled off, and each piece was mounted for sectioning with the ultramicrotome. Thin sections were collected on formvar-coated slotted grids and sometimes stained with lead citrate and uranyl acetate.

Fiber reconstructions

Single fibers were first reconstructed from serial sections using a light microscope and drawing tube at a total magnification of 312×. Then, each primary collateral, its ramifications, and terminal endings were drawn using a magnification of 1,250×. The piece-by-piece reconstruction of labeled fibers was performed by matching fiber segments and blood vessels on the cut surfaces of adjacent sections. Continuity of the labeled fiber could be determined with a high degree of confidence since there were very few labeled fibers in any single section. All fiber reconstructions in the present report are shown as if they were obtained from a right cochlear nucleus. Thus, fibers from the left side have been deliberately reversed.

Matching units to fibers

A number of factors were considered in order to match a reconstructed fiber with the proper physiological unit. In the best cases (26 fibers), the anterior-posterior and dorsal-ventral (depth) position of a fiber's trajectory within the nerve matched the estimated position of the pipette tip at the time of injection. From these cases, unit CF correlated closely with the relative spatial position of the fiber within the cochlear nucleus, and staining intensity appeared related to the injection parameters of current amplitude and duration. Since only a few units were injected during any experiment, and these were intentionally well separated in CF, we identified an additional 11 fibers based on staining characteristics and the relative position of the fiber in the cochlear nucleus.

Completeness of staining

Quantitative measures were collected only from fibers that appeared to be darkly stained throughout their arbors. For such fibers (n = 27), every axonal collateral gave rise to a distinct swelling (98%) or terminated abruptly (2%). These distinct terminations provide the best light-microscopic evidence that the entire fiber was filled with HRP. These fibers could be easily distinguished from cases where the reaction product gradually became fainter with increasing distance from the injection site. There were eight fibers for which such progressive fading was confined to the descending branch within the dorsal cochlear nucleus (DCN). Since the collaterals within the ventral cochlear nucleus (VCN) were darkly labeled, the ascending branches were maintained as part of the descriptive data base.

Even in darkly labeled fibers, HRP reaction product in the thickly myelinated parent axons could be faint or undetectable for short stretches in the middle of a section. Such staining anomalies of the thickest axons were primarily evident within the auditory nerve and the zone of bifurcations. Thinner collaterals in this region were always darkly stained, and the heavily myelinated axons were darkly stained at nodes of Ranvier (Fig. 3). The data suggest that the penetration of the highly polar chromogen (DAB) necessary for the formation of the intracellular reaction product is especially impeded by myelin, since the degree of fading in the depth of the section depends upon the extent to which the labeled axon is myelinated. This penetration artifact should not affect the present results

Fig. 2. Reconstruction of a right cochlear nucleus in the "modified sagittal" plane. The angle of this plane is shown schematically by the coronal section in the lower right. Left column: representative block model sections illustrate the major subdivisions of the cochlear nucleus. With the aid of a computer, the block model (Kiang et al., '75) was rotated and resectioned to match tissue sections. The axes are in block model units (BMU); one BMU equals 80 μm. Each section is indicated by its percent distance through the cochlear nucleus, with the lateral extreme defined as 0% and the medial extreme as 100%. Upper right: diagrammatic representation of the procedure used to construct the orientation diagrams shown in subsequent figures. For each brain, the maximal extent of the dorsal cochlear nucleus (DCN) is obtained from more lateral sections (here outlined from the 20% interval with the granule cell area omitted), and the maximal outline of the ventral cochlear nucleus (VCN) is sampled from more medial sections (60% interval in this case). When superimposed in two dimensions, the DCN and VCN overlap considerably in the posterior half of the nucleus. The boundary line is approximately the average of this overlap. When diagramming single fibers, we attempt to maintain as accurately as possible the position of the boundary with respect to the fiber. That is, a given collateral will appear in the division appropriate to its actual location (DCN or VCN). Lower right: coronal section indicating the angle of the "modified sagittal" plane. Percentages refer to the block model planes shown on the left. Abbreviations: A, anterior; a, anterior division of AVCN; AS, acoustic striae; AVCN, anteroventral cochlear nucleus; C, central region of PVCN; DM, dorsomedial; FCL, fusiform cell layer of DCN; G, granule cell layer; ICP, inferior cerebellar peduncle; ML, molecular layer of DCN; PD, posterodorsal part of AVCN; PL, polymorphic layer of DCN; PV, posteroventral part of AVCN; PVCN, posteroventral cochlear nucleus; r, remainder of PVCN; SOC, superior olivary complex; V, spinal trigeminal nucleus.

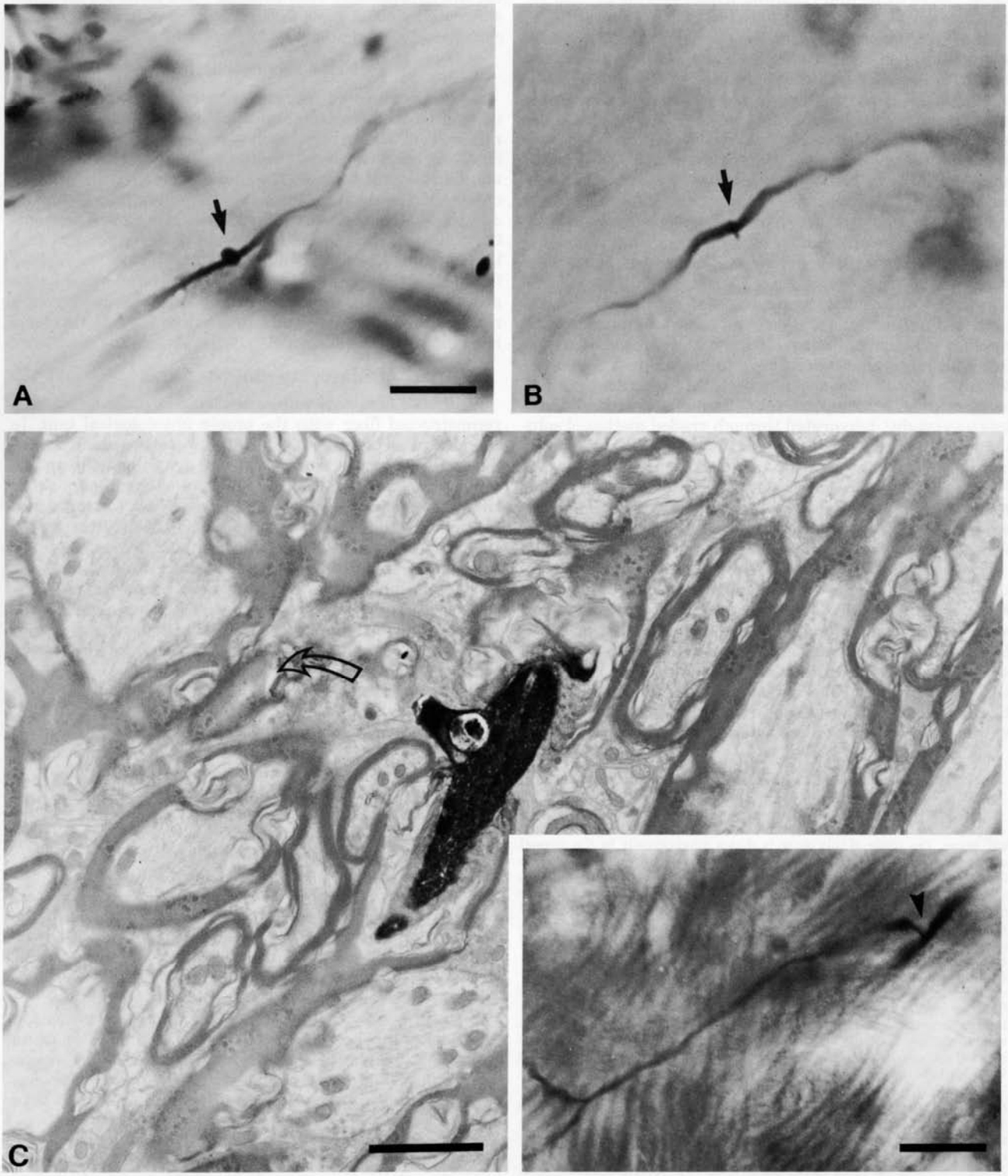

Fig. 3. Variation in the intensity of the HRP reaction product along individual axons. Light micrographs in panels A and B illustrate presumed nodes of Ranvier (arrows). Note that the HRP reaction product fades on either side of the nodes. The electron micrograph in panel C illustrates an HRP-filled branch point (arrowhead, inset). The axon loses its myelin at the point where the collateral emerges, and the collateral staining is much darker than that in adjacent parts of the parent fiber (inset). A portion of the myelin surrounding the collateral is indicated by the curved arrow. Magnification of A and B is the same, scale bar in A = 20 μm, scale bar in C = 1 μm. Scale bar in the inset of C = 20 μm.

TABLE 1. Means, Standard Deviations, and Statistical Comparisons

	High SR (n = 15)	Low/Med SR (n = 12)	Total (n = 27)	p Values (high vs. low/med SR)
Number of primary collaterals				
Total	20.3 ± 4.45	21.4 ± 4.55	20.8 ± 4.53	n.s.
Root branch	0.8 ± 1.05	1.3 ± 1.89	1.0 ± 1.50	n.s.
Ascending branch (AB)	8.6 ± 2.60	9.2 ± 2.45	8.9 ± 2.56	n.s.
Descending branch (DB)	10.9 ± 3.15	10.8 ± 2.82	10.9 ± 3.01	n.s.
Number of branch points				
Total	56.5 ± 20.03	96.6 ± 44.46	74.3 ± 38.70	$p<.01$
Root branch	3.3 ± 4.86	6.9 ± 10.59	4.8 ± 8.11	n.s.
Ascending branch	24.0 ± 11.23	52.7 ± 33.12	36.7 ± 27.58	$p<.01$
Descending branch	29.3 ± 11.89	36.9 ± 15.99	32.7 ± 14.37	n.s.
Parent lengths (mm)				
Total (AB + DB)	5.75 ± 0.75	5.64 ± 0.67	5.70 ± 0.72	n.s.
Root branch	0.89 ± 0.66	1.14 ± 1.08	0.98 ± 0.84	n.s.
Ascending branch	2.32 ± 0.35	2.33 ± 0.68	2.33 ± 0.53	n.s.
Descending branch	3.43 ± 0.66	3.31 ± 0.60	3.38 ± 0.64	n.s.
Collateral lengths (mm)				
Total	7.01 ± 1.76	9.93 ± 3.77	8.31 ± 3.19	$p<.02$
Root branch	0.56 ± 0.87	0.89 ± 1.47	0.71 ± 1.19	n.s.
Ascending branch	2.79 ± 1.09	5.06 ± 2.89	3.80 ± 2.38	$p<.02$
Descending branch	3.65 ± 1.46	3.98 ± 1.38	3.80 ± 1.43	n.s.

because collaterals, branch points, and terminal endings are thinly myelinated or unmyelinated.

Data analysis

Drawing tube tracings were digitized and fiber lengths determined using a computerized planimeter. Parent axons were measured from low-magnification (312×) drawings; because these segments tended to have relatively straight trajectories, their lengths were corrected for depth of travel through the series of sections using the Pythagorean theorem. Collateral lengths and branch point counts were determined from high-magnification (1,250×) reconstructions. Since the collaterals tend to have complex trajectories within the thickness of a single section, the length measures were left uncorrected. All quantitative results (means, standard deviations, and Student's t-test p values) are listed in Table 1.

Each unit was assigned a CF as defined by the preinjection tuning curve, and then placed in one of three functional groups (criteria of Liberman, '78 based on its SR prior to the HRP injection: low SR units discharged at rates less than 0.5 spikes/second, medium SR units had rates between 0.5 and 18 spikes/second, and high SR units had rates exceeding 18 spikes/second. Because our sample is small, and because low and medium SR fibers tend to share many morphological features (present results; see also Liberman, '82a), they have been grouped together for purposes of statistical comparisons (t-test) to high SR fibers.

RESULTS

General description and nomenclature

The fibers in this study range in CF from 0.17 kHz to 40 kHz, and in SR from near zero to 102 spikes/second (Fig. 4). The fiber reconstruction in Figure 5 illustrates several features common to most of the fibers in the sample. The "root branch" crosses the Schwann-glial border, ascends into the cochlear nucleus, and bifurcates. At the "bifurcation," the axon is thinner in diameter. This characteristic bifurcation gives rise to an "ascending branch" and a "descending branch." The ascending branch is directed anteriorly through the anteroventral cochlear nucleus (AVCN) and the

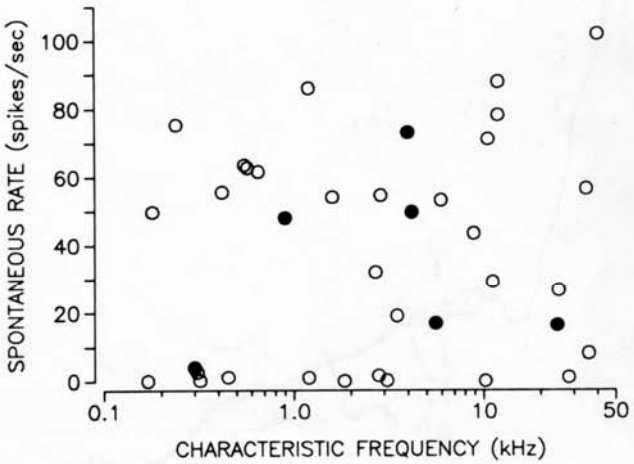

Fig. 4. Plot illustrating the CF and SR for each fiber (n = 37) in the present sample. Open circles correspond to those fibers which innervate the DCN; filled circles correspond to fibers which fail to project into the DCN.

descending branch is directed posteriorly through the posteroventral cochlear nucleus (PVCN), toward and usually into the DCN. The ascending, descending, and root branches maintain generally straight trajectories, have the largest average diameters, and are referred to as "parent" branches.

Along the parent branches, nodes of Ranvier can be observed at relatively regular intervals (also see Liberman and Oliver, '84). "Primary collaterals" arise at nodes, are generally thinner in diameter, and exhibit trajectories shorter than and roughly orthogonal to that of their parent branch. Nodal constrictions are generally not detectable on the thinner collateral branches. The number of primary collaterals arising from the parent branches ranges from 14 to 30 per fiber and appears unrelated to CF or SR. The primary collaterals branch a variable number of times to yield the axonal arbor. As an indicator of arbor complexity, we counted the number of branch points per fiber (Fig. 6A)

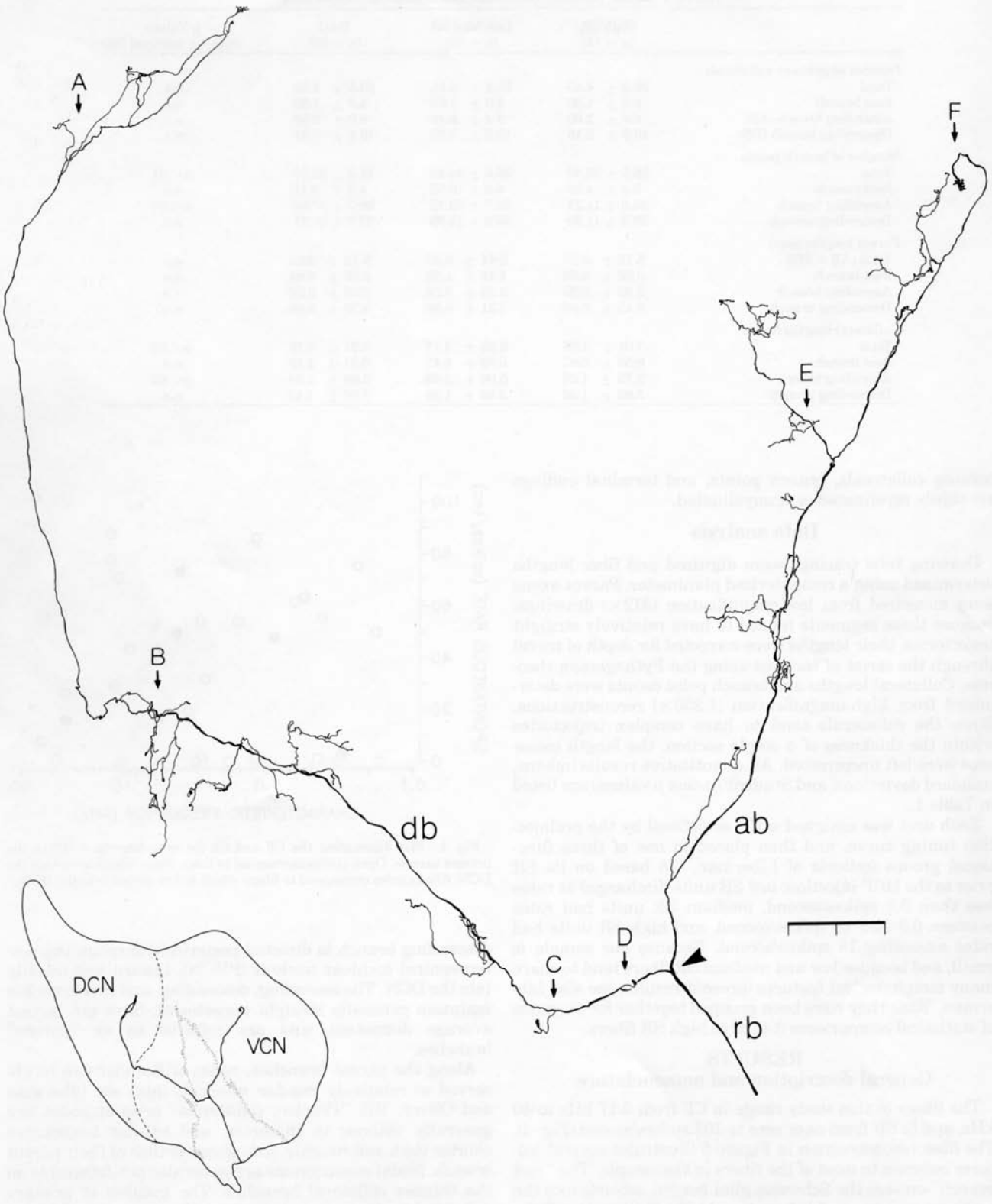

Fig. 5. Drawing-tube reconstruction (original total magnification × 312) of a single auditory nerve fiber (CF = 11.6 kHz, SR = 29 spikes/second). For this and subsequent drawing-tube reconstructions, anterior is toward the right and dorsomedial is toward the top. Upon entering the cochlear nucleus, the root branch (rb) bifurcates (arrowhead) to form the ascending (ab) and descending (db) branches. The parent axons give rise to 22 primary collaterals. Several of these (A–F) are shown in more detail in Figure 7. Inset shows the position of the parent axons with respect to the major divisions of the cochlear nucleus. Scale bar = 200 μm.

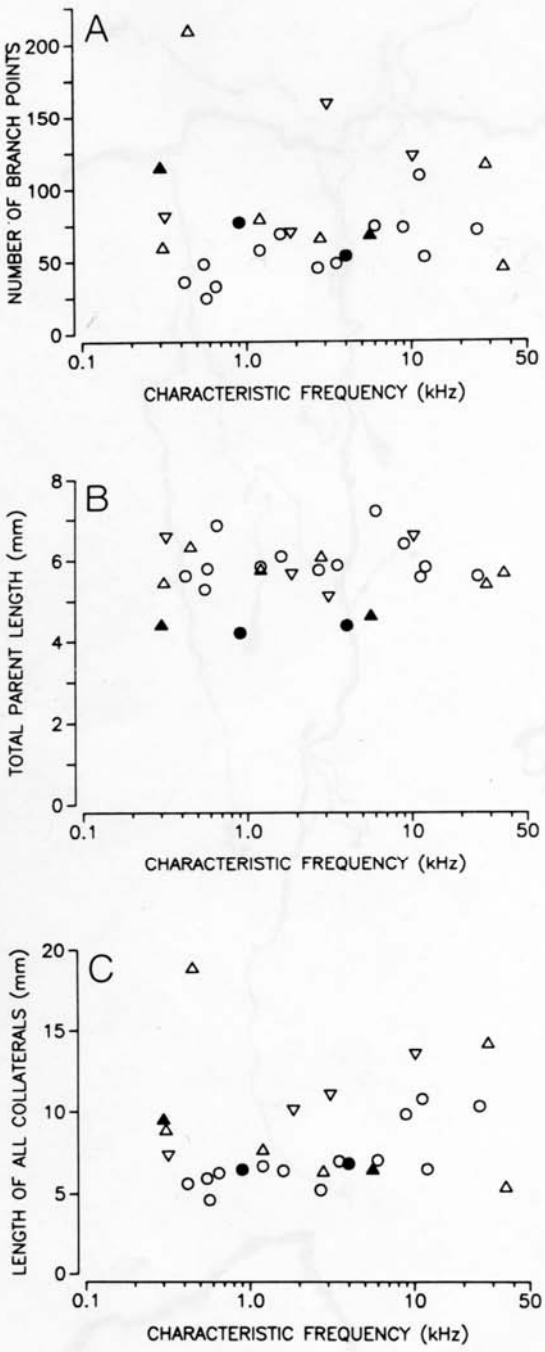

Fig. 6. Plots of quantitative anatomical features for 27 darkly labeled fibers as a function of the physiological properties of CF and SR. A. The number of branch points, excluding the bifurcation, for collaterals arising from the root, ascending, and descending parent branches of each fiber. B. The combined length of the ascending and descending parent axons. C. The summed length of all collateral arborizations along the root branch, the ascending branch, and the descending branch. Symbols: (▽), SR below 0.5 spikes/second; (△), SR between 0.5 and 18 spikes/second; (○), SR above 18 spikes/second. Open symbols correspond to fibers which innervate the DCN, PVCN, and AVCN; filled symbols denote fibers which do not project to the DCN.

and found that low and medium SR fibers have on average 70% more branch points than do high SR fibers (Table 1). Furthermore, the total length of the collaterals for low and medium SR fibers is approximately 40% greater on average than that of high SR fibers (Table 1, Fig. 6C). In contrast, the combined length of ascending and descending parent branches appears unrelated to fiber CF or SR (Fig. 6B).

Distinct swellings are frequently observed along the more distal segments of the thinner collateral branches. Such swellings may be boutons en passant as described by Peters et al. ('76). En passant swellings are not observed on all collaterals, but when present, they tend to occur in groups linked together by short filamentous segments. Visible swellings also characterize the tips of collateral ramifications. The morphology of these terminal swellings (or endings) can vary markedly in size and shape along a single fiber, ranging from the very large endbulbs of Held to small simple boutons (Fig. 7).

Root branch

The spatial distribution of auditory nerve fibers in the cochlear nucleus is such that fibers having sequentially higher CFs bifurcate at progressively more dorsal regions of the nucleus. From the bifurcation, fibers maintain their relative dorsoventral positions throughout the cochlear nucleus. The position of the bifurcation was quantified by measuring the length of the root branch (Fig. 8). This length can be reliably defined since the junction between nerve and nucleus is marked by a sharp transition in the type of satellite cells ensheathing the axons and can be easily localized in histological sections. The data in Figure 8 show a strong correlation ($r = .95$, $p < .001$) between the length of the root branch and CF. The length of the root branch does not appear related to SR (Fig. 9B).

One exception to the relationship between CF and length of the root branch is a high CF fiber which has its bifurcation in the auditory nerve, apparently peripheral to the Schwann-glial border (Fig. 10). Although the position of the bifurcation is grossly inappropriate for the CF of this fiber (30 kHz), the ascending and descending branches continue in a parallel trajectory with other root branches for over 2.7 mm until they reach the appropriate high-frequency regions of the cochlear nucleus. They then diverge from one another and thereafter display apparently normal topographic projections.

Root branch collaterals can arise at or prior to bifurcation (Fig. 11), although these collaterals are not present on all fibers. These primary collaterals are distinctly thinner than the parent branch and consequently their branch points are not confused with the bifurcation. Their numbers, lengths, and additional branchings vary greatly across fibers, but even the most complex root collaterals tend to be restricted to the zone of bifurcations. Root branch collaterals range in number from zero to six and are more common among fibers of high CF (correlation coefficient = .65, $p < .01$). Collaterals from fibers of lower CFs (below around 5 kHz) generally conform to projection planes established by their respective ascending and descending branches. In contrast, those from fibers of higher CFs tend to ramify across many projection planes, especially those generated by fibers of lower CFs. CF is also correlated with the number of branch points and the summed length of collaterals arising from the root branch (Fig. 9). When these features are compared across SR groups, they do not show statistically significant differences. Because less than half of the fibers display root

Fig. 7. Selected collaterals traced at an original total magnification of ×1,250 from the primary fiber illustrated in Figure 5. A. Simple bouton endings and en passant swellings arise from thin collaterals in the polymorphic layer of the DCN. B. Long, ventrally directed collaterals terminate as boutons of varying size in the central region of the PVCN. C,D. Complex endings terminate in the vicinity of cell bodies (not shown) corresponding in morphology to the globular cells (Osen, '69). E. En passant swellings and terminal boutons end either in the neuropil or on the soma of neurons in the AVCN. F. Large axosomatic endbulb of Held terminates in the anterior division of the AVCN.

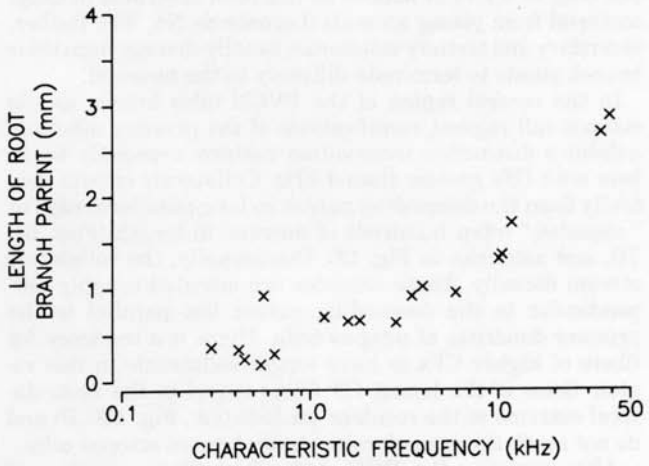

Fig. 8. Length of the root branch parent as a function of CF. This plot includes some fibers which faded after entering the DCN. All fibers were identified by a correspondence between their trajectory in the nerve and the estimated position of the electrode tip during iontophoresis.

branch collaterals, and because of the strong CF effect, it is difficult to draw conclusions from the absence of SR effects.

Descending branch

Representative examples of descending branches are shown in Figure 12. Of the 37 fibers in our sample, 31 innervate both the ventral and the dorsal cochlear nuclei (open circles of Fig. 4, 6, 9, 14, 16). The remaining six fibers innervate the VCN, but do not project into the DCN (closed circles). One fiber in our sample appears to lack a descending branch; a bifurcation is present (arrowhead) but both major branches are directed anteriorly (Fig. 13). Those fibers which fail to innervate the DCN are among the most darkly labeled fibers in our sample, and the tips of all their collaterals are marked by distinct terminal swellings. In addition, postinjection survival times for those fibers that innervate the DCN ($\bar{x} = 28.0 \pm 2.6$; range = 23–31.5 hours) and those that do not ($\bar{x} = 26.9 \pm 2.8$; range = 23–31 hours) are essentially identical. Within a cat, fibers failing to innervate the DCN did not correspond to those having the shortest survival times. Therefore fading of the HRP reaction product or incomplete filling is not a likely explanation for this innervation difference. Neither CF nor SR is correlated with innervation of the DCN.

It is difficult to define an end to the descending parents since they progressively diminish in diameter as they course posteriorly. Usually, the parent branch arborizes into a series of fine terminal collaterals (Fig. 12A). Occasionally, the thinning parent simply terminates as a single bouton. In other cases, the parent fiber bifurcates in the PVCN or DCN (double arrows, Fig: 12B,C), but the parent and major collateral continue their trajectory parallel to one another, often terminating within 100 μm of each other. A fourth pattern is that the parent fiber breaks up into a dense terminal arbor, with none of the collateral branches continuing in the same direction or with the same caliber as the parent (Fig. 12D). For purposes of length measurements, the descending branch parent is defined as terminating at the most posterior ending emitted at the distal extreme of the fiber (arrows in Fig. 12).

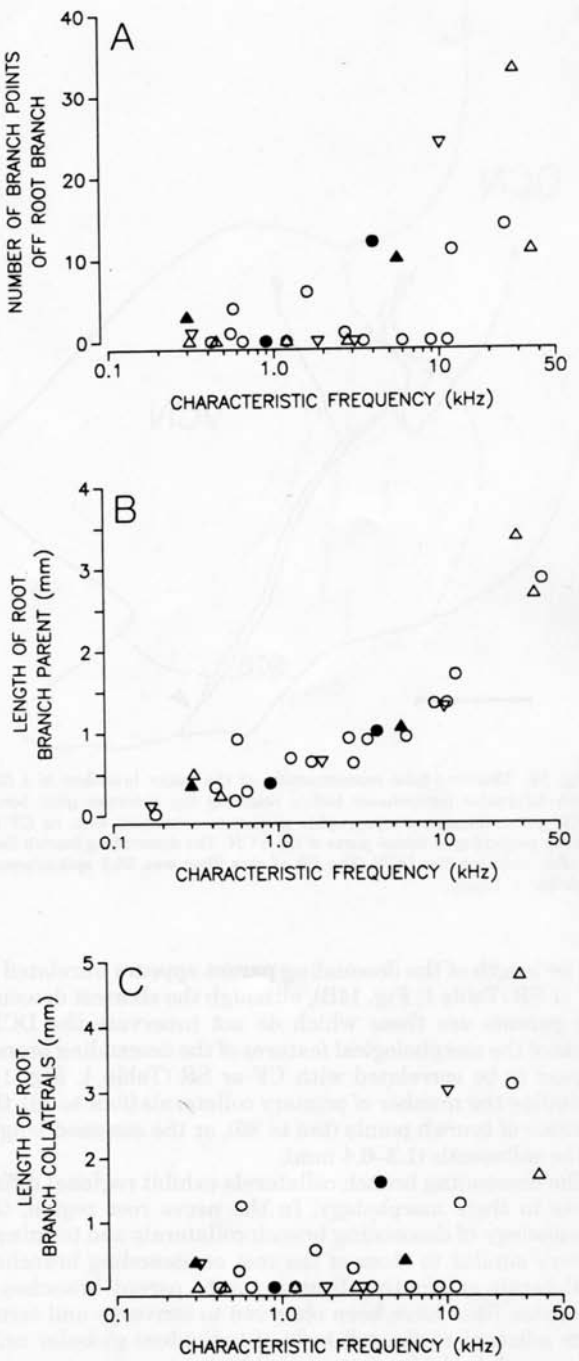

Fig. 9. Morphometry of the root branch. A. The number of branch points arising from the root branch and its collaterals is correlated with CF (correlation coefficient = .68, $p < .01$). B. The length of the root branch parents (n = 26) which could be continuously traced to the Schwann-glial border is correlated with CF (correlation coefficient = .94, $p < .01$). The sample in this figure overlaps only partially with the 27 fibers used for other quantitative measures and includes fibers that faded after entering the DCN. C. The total length of the collateral arborization arising from the root branch is correlated with CF (correlation coefficient = .73, $p < .01$). Symbols are the same as in Figure 6.

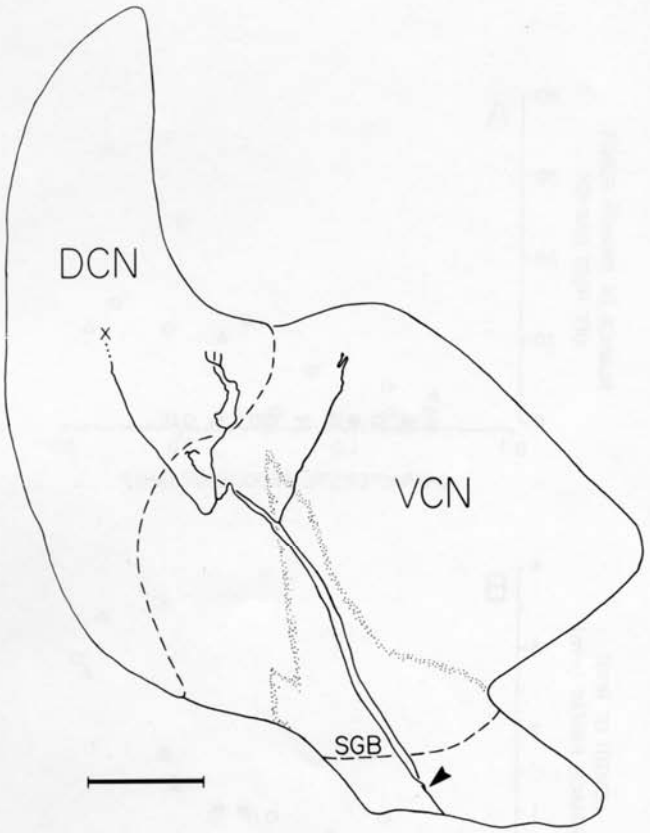

Fig. 10. Drawing tube reconstruction of the major branches of a fiber which bifurcates (arrowhead) before reaching the Schwann-glial border (SGB), yet maintains a topographic projection consistent with its CF (30 kHz) by projecting to dorsal parts of the VCN. The descending branch fades (x) after entering the DCN. The SR of this fiber was 56.3 spikes/second. Scale bar = 1 mm.

The length of the descending parent appears unrelated to CF or SR (Table 1, Fig. 14B), although the shortest descending parents are those which do not innervate the DCN. None of the morphological features of the descending branch appear to be correlated with CF or SR (Table 1, Fig. 14), including the number of primary collaterals (four to 16), the number of branch points (ten to 80), or the summed length of the collaterals (1.3–6.4 mm).

The descending branch collaterals exhibit regional differences in their morphology. In the nerve root region, the morphology of descending branch collaterals and terminals is very similar to those of the root or ascending branches. Collaterals originating from separate parent branches of the same fiber have been observed to converge and terminate adjacent to the cell body of individual globular cells. In general, both simple terminal boutons and complex terminal endings are formed by descending branch collaterals in the posteroventral part of the AVCN (Fig. 7C,D). In a few instances we have observed complex endings arising from the descending branch which are of sufficient size to conform to the description of endbulbs of Held.

All descending parent branches appear to ramify as they pass through the multipolar cell area of the PVCN. Collateral arborizations give rise primarily to en passant swellings and simple boutons. It is noteworthy that no single fiber in our sample forms a "pericellular nest" around the cell body of a PVCN neuron as has been described in Golgi material from young animals (Lorente de Nó, '81). Rather, secondary and tertiary collaterals usually diverge from their branch points to terminate diffusely in the neuropil.

In the central region of the PVCN (also known as the octopus cell region), ramifications of the primary afferents exhibit a distinctive innervation pattern, especially for fibers with CFs greater than 4 kHz. Collaterals stream ventrally from the descending parent in long parallel arrays or "cascades," often hundreds of microns in length (Figs. 5B 7B, and asterisks in Fig. 12). Occasionally, the collaterals stream dorsally. These cascades are oriented roughly perpendicular to the descending parent but parallel to the primary dendrites of octopus cells. There is a tendency for fibers of higher CFs to have longer collaterals in this region. Some of the lowest CF fibers travel in the ventrolateral extreme of the cochlear nucleus (i.e., Fig. 12C,D) and do not reach the more dorsomedially located octopus cells.

After entering the DCN, individual fibers ramify and terminate within a narrow band of the deep polymorphic layer, and only an occasional collateral reaches as far as the fusiform cell layer. No labeled terminals were observed in the molecular layer. The parent axon greatly diminishes in diameter after entering the DCN and only a few fine collaterals (often less than 0.5 μm in diameter) are emitted from a single fiber. Collateral ramifications are sparse and terminate as small simple boutons (Fig. 5A, 7A, 12A,C). In the DCN, en passant swellings and terminal boutons were found primarily in the neuropil; they were rarely observed in the immediate vicinity of a cell body. The topographic banding of terminal arbors in the DCN is consistent with the tonotopic arrangement of this nucleus (Rose et al., '59).

Ascending branch

The parent ascending branch was considered by Ramón y Cajal ('09) to terminate at its most anterior endbulb of Held, and this criterion could be used to define the ascending branch parent for all but one fiber in the sample. The exception is an ascending branch that terminates as a series of boutons in the posterior division of the AVCN; no endbulb of Held is apparent. This fiber is the only one in our sample which does not project into the anterior division of the AVCN. For all other fibers, the ascending parent maintains a relatively straight trajectory into the anterior division of the AVCN, and terminates as a large endbulb of Held (arrows, Fig. 15). By this definition, the end of the ascending parent is not necessarily the most anterior portion of a fiber.

The length of the ascending branch parent, although more variable for fibers of low CFs, appears unrelated to either CF or SR (Fig. 16B). On average, the number of primary collaterals on the ascending branch (ranging from four to 16) is less than that for the descending branch and also does not appear related to CF or SR. In contrast, the overall complexity of the ascending branch arbor is strongly correlated with SR. The number of branch points for low and medium SR fibers is, on average, more than twice that for high SR fibers (Fig. 16A). In addition, the mean collateral length for low and medium SR fibers is 80% greater than that for high SR fibers (Table 1, Fig. 16C). The most elaborate branching pattern in the present sample is from the medium SR fiber (total collateral length of 12.5 mm) shown in Figure 15C.

The data on lengths of the root and ascending parents can be combined with data from a previous study to estimate

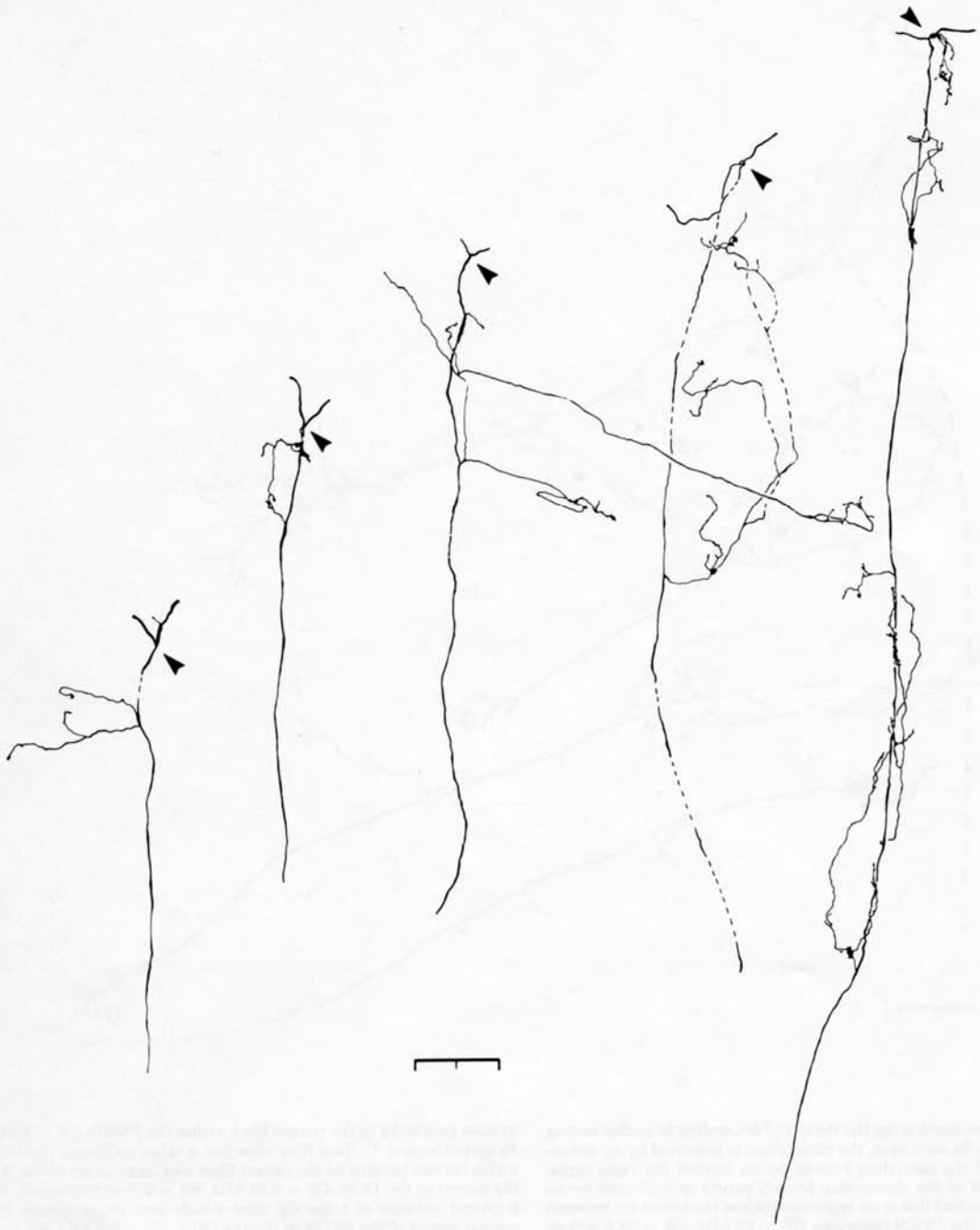

Fig. 11. Drawing-tube reconstructions (original magnification ×1,250) of the root branch segment of five fibers which display root collaterals. The root branches are arranged in order of increasing CF. From left to right, the CFs (in kHz) of the fibers are 0.57, 4.2, 10.6, 25, and 28.2. From the point of bifurcation (arrowhead), the stumps of ascending branches are directed toward the right. Scale bar = 200 μm.

the total length of single auditory nerve fibers, from the organ of Corti to the most anterior endbulb of Held (Fig. 17). The data are preliminary, but they clearly suggest that the difference in the lengths of root branches compensates for the difference in intracochlear lengths (Liberman and Oliver, '84), to the extent that the total lengths of the low and high CF fibers are quite similar. This conclusion is in agreement with that reached by fine dissection of the auditory nerve (Arnesen and Osen, '78).

The collateral ramifications of most ascending branches are short and relatively simple, especially those of high SR fibers. The relative thickness of terminal collaterals roughly corresponds to the size of the terminal endings. For fibers with multiple endbulbs, the most anterior endbulb is usu-

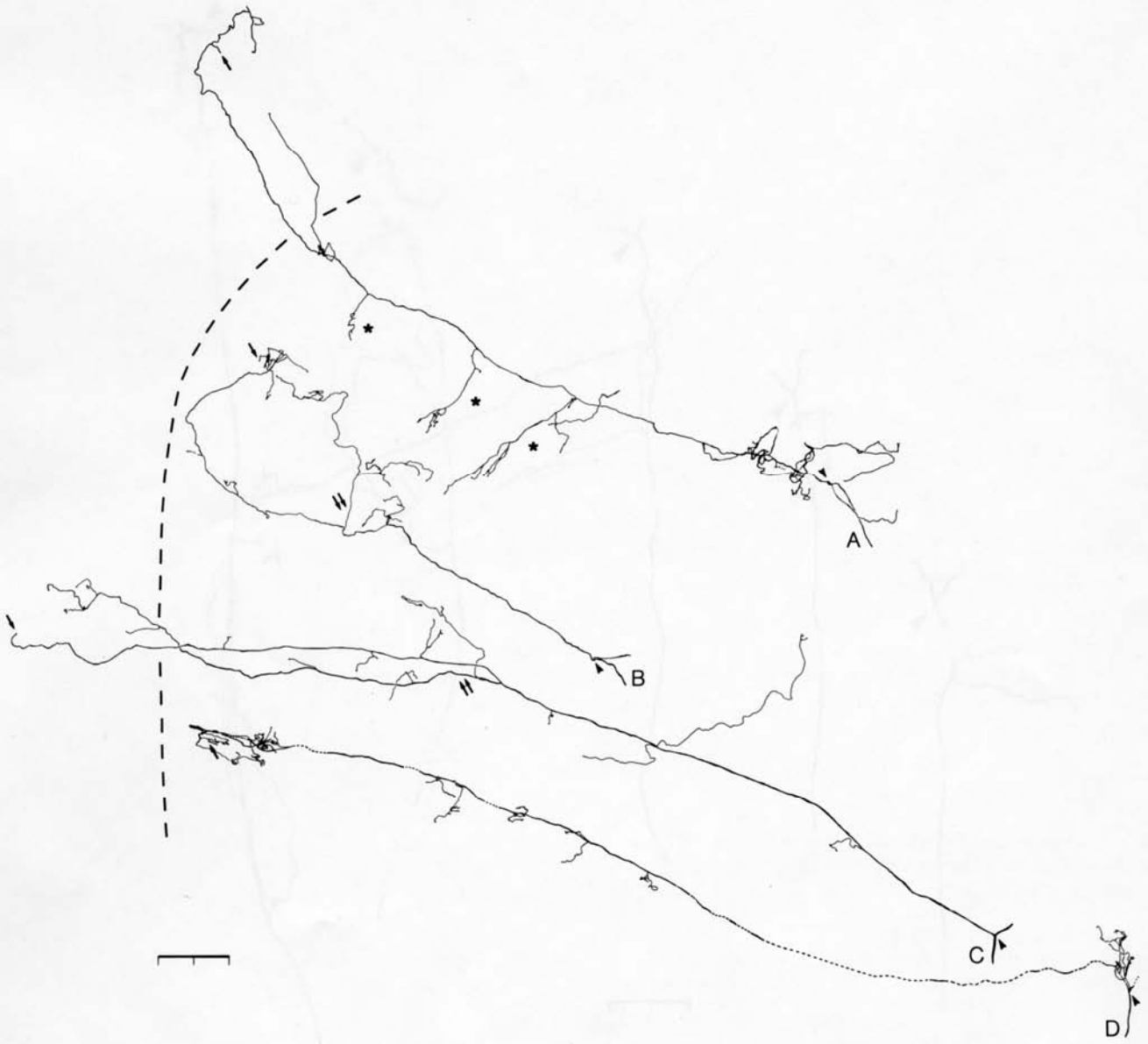

Fig. 12. Examples illustrating the variety of descending branches among our present sample. In each case, the bifurcation is indicated by an arrowhead, the stump of the ascending branch points toward the right (anteriorly), and the end of the descending branch parent is indicated by an arrow. The heavy dashed line is an approximation of the boundary between the DCN (left) and the PVCN (asterisk). CF = 25 kHz, SR = 26.5 spikes/second. B. This fiber has a large collateral (double arrows) which terminates in close proximity to the parent fiber within the PVCN. CF = 4 kHz, SR = 73 spikes/second. C. This fiber also has a large collateral (double arrows) which travels parallel to the parent fiber and terminates within 200 μm of the parent in the DCN. CF = 0.31 kHz, SR = 2.7 spikes/second. D. This is a typical example of a low CF fiber which does not innervate either the central region of the PVCN or the the DCN. CF = 0.3 kHz, SR = 4 spikes/second. Scale bar = 200 μm.

ally the largest and located in the anterior division of the AVCN; en passant and simple terminal endings are also found in this region. Complex terminal endings (including smaller endbulbs), simple terminal endings, and en passant endings are found in the posterior division of the AVCN.

The spatial distribution and overall curvature of individual ascending branch ramifications correspond roughly with the tonotopic (Rose et al., '59; Bourk et al., '81) and cochleotopic (Sando, '65; Osen, '70) maps for the AVCN. Nearly two-thirds of the ascending branches define relatively narrow projection planes within the dorsoventral and mediolateral dimensions. Collaterals and terminals typically remain within a few hundred microns of the parent ascending branch (Fig. 15A). In three of these cases, the ascending branch parent appears to split in the posterior division of the AVCN. Both branches are of large diameter, continue anteriorly to terminate as large endbulbs of Held, and conform to an isofrequency projection plane by distributing themselves along the mediolateral dimension. An example is shown in Figure 15B (double arrows). All fibers display-

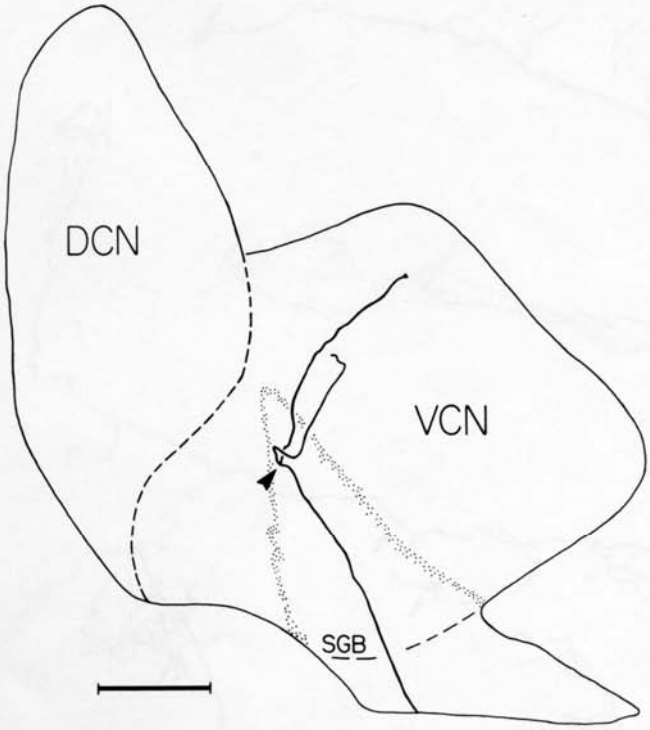

Fig. 13. Drawing tube reconstruction of the major branches of a fiber which has no descending parent. This fiber was not included in the morphometric analyses because of its unusual morphology. CF = 24.5 kHz, SR = 16.3 spikes/second. Scale bar equals 1 mm.

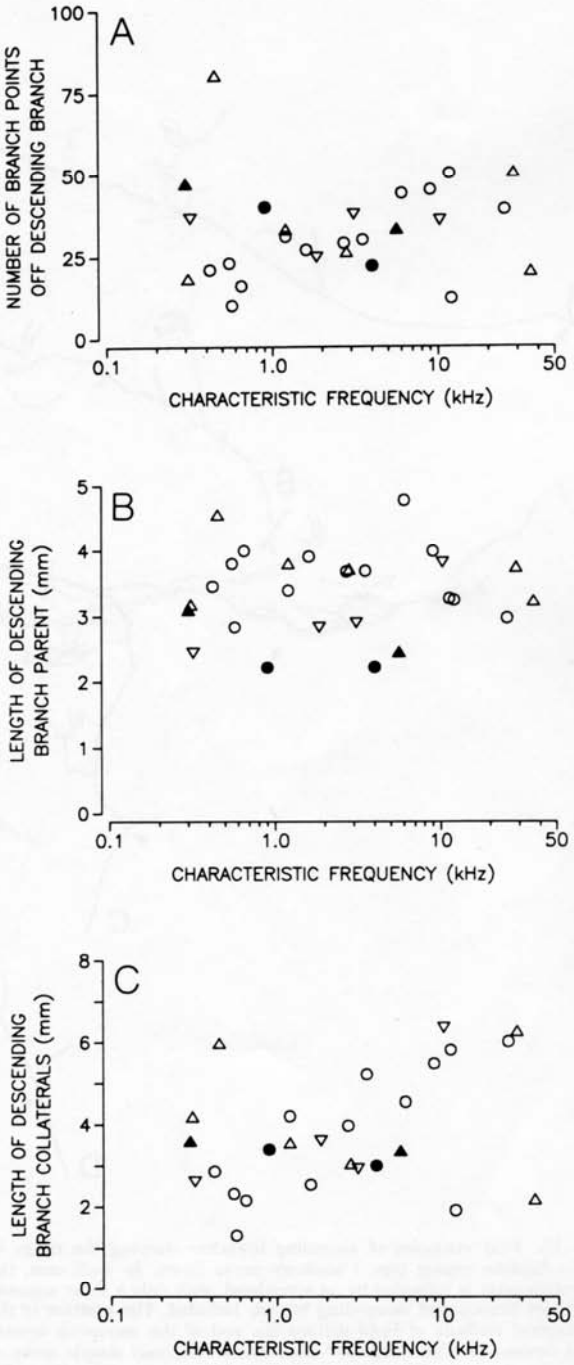

Fig. 14. Morphometry of the descending branch. A. The number of branch points arising from the descending branch. B. The length of the descending branch parent axon. C. The total length of the collateral arborization arising from the descending branch. Symbols are the same as in Figure 6.

ing two major ascending branches have CFs below 0.5 kHz, although not all fibers below 0.5 kHz exhibit this morphology. The remaining one-third of the fibers have ascending branches with more complex arbors and wider projection planes. These fibers have long collaterals directed either anteriorly (double arrowhead, Fig. 15C), or laterally (crossed arrows, Fig. 15C,D). In many cases these collaterals appear to deviate from the usual laminar organization of isofrequency contours, usually by an extended projection in the dorsal direction. Such collaterals generally terminate in the extreme peripheral zones of the AVCN.

DISCUSSION

Classification schemes based on morphology

The central projections of the neurons in this study are similar in many respects to the classical descriptions of kitten material prepared by the Golgi technique (Held, 1893; Kölliker, 1896; Ramón y Cajal, '09; Lorente de Nó, '81). After crossing the Schwann-glial border, each fiber bifurcates in a position consistent with its CF and gives rise to an ascending and a descending branch. Numerous collaterals are emitted along the course of each fiber, and they terminate in a variety of ending formations.

Even in our limited sample, however, we have found significant variations on this basic theme. For example, 16% of the fibers (6/37) do not project into the DCN. Differential innervation of major cytoarchitectonic subdivisions in the VCN, including the small cell cap, is also evident. Our sample size is too small to interpret the possible significance of these and other more subtle morphological differences, although we know that they do not appear to be strongly correlated with either CF or SR.

The classical view suggesting that every auditory nerve fiber sends terminals to every subdivision of the cochlear nucleus (as was originally implied by Lorente de Nó, '33)

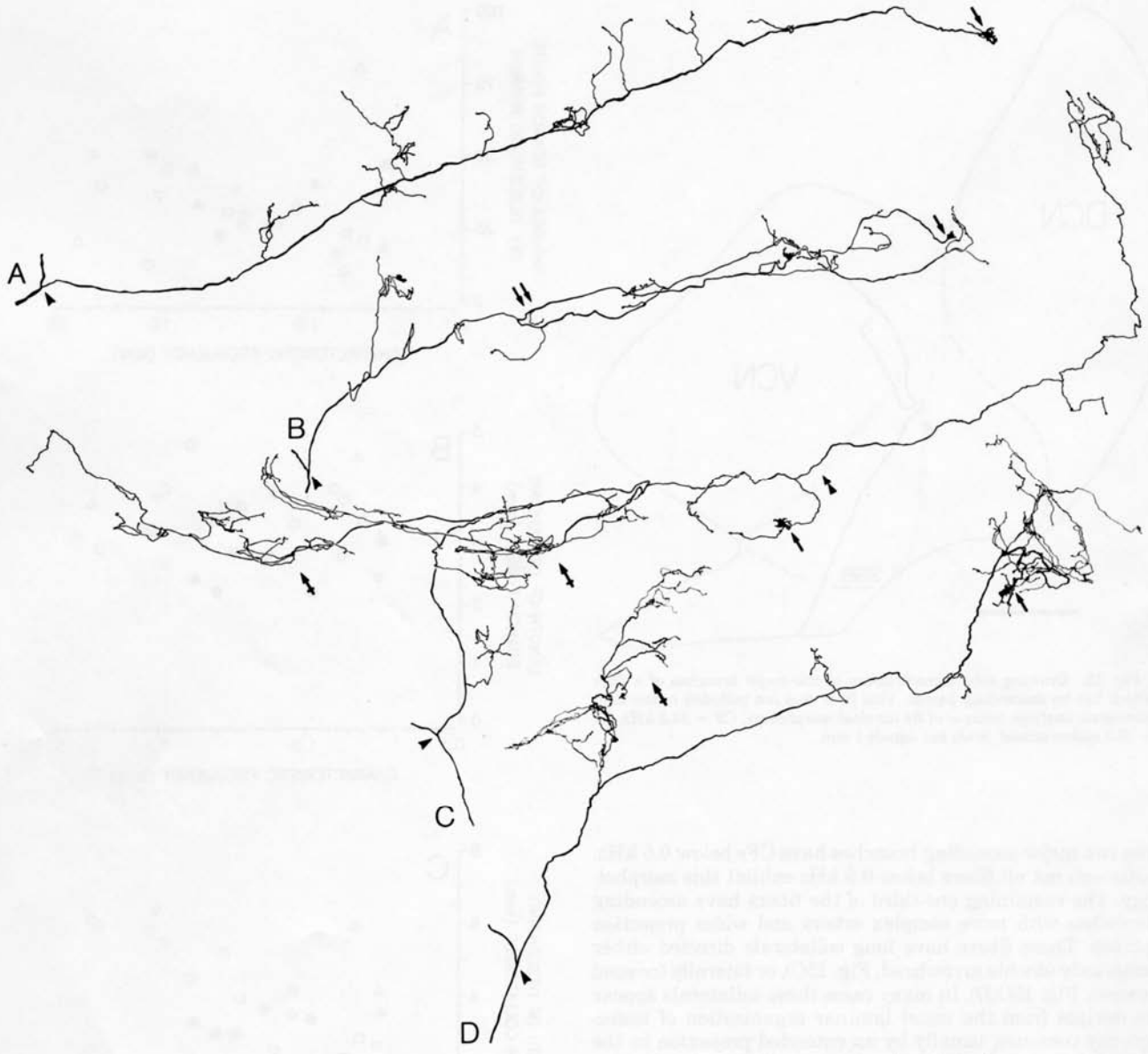

Fig. 15. Four examples of ascending branches showing the range in collateralization among type I auditory nerve fibers. In each case, the bifurcation point is indicated by an arrowhead, with only a short segment of the root branch and descending branch included. The position of the anteriormost endbulb of Held defines the end of the ascending branch parent (arrow). A. This "regular" fiber has a relatively simple array of collaterals all terminating within a restricted projection plane. CF = 2.8 kHz, SR = 1.6 spikes/second. B. This fiber displays a large, ascending collateral (double arrows) which travels parallel to the parent axon and also gives rise to an endbulb. CF = 0.24 kHz, SR = 75 spikes/second. C. This fiber has a long, thin collateral emanating from the end of the ascending parent (double arrowheads) to terminate in the anterior extreme of the AVCN among small neurons. In addition, this fiber innervates small cells in the lateral extreme of the AVCN by two collaterals emitted in the nerve root region (crossed arrows). CF = 0.45 kHz, SR = 1.2 spikes/second. D. This fiber has a long dorsolaterally directed collateral (crossed arrow) which fails to conform to a narrow isofrequency plane within the AVCN. CF = 3.1 kHz, SR = 0.2 spikes/second. Scale bar = 200 μm.

needs revision. In fact, Lorente de Nó's more recent publication ('81) describes three groups of fibers based on morphological differences among ascending branches. His group A fibers give rise to chalices (endbulbs) of Held which terminate in the rostral pole of the anterior division of the AVCN, but not in the posterior division (similar to Fig. 15A). Group B fibers have endbulbs which terminate more posteriorly in the AVCN and innervate more anterior regions only by means of long thin collaterals ending as boutons (similar to Fig. 15C). Group C fibers apparently have only "rudimentary" endbulbs, or none at all, yet they display extensive collateral and terminal ramifications. These varieties of ascending branching have also been described by other investigators (Feldman and Harrison, '69; Brewar and Morest, '75). Lorente de Nó speculates that group A, B, and C fibers correspond, respectively, to the

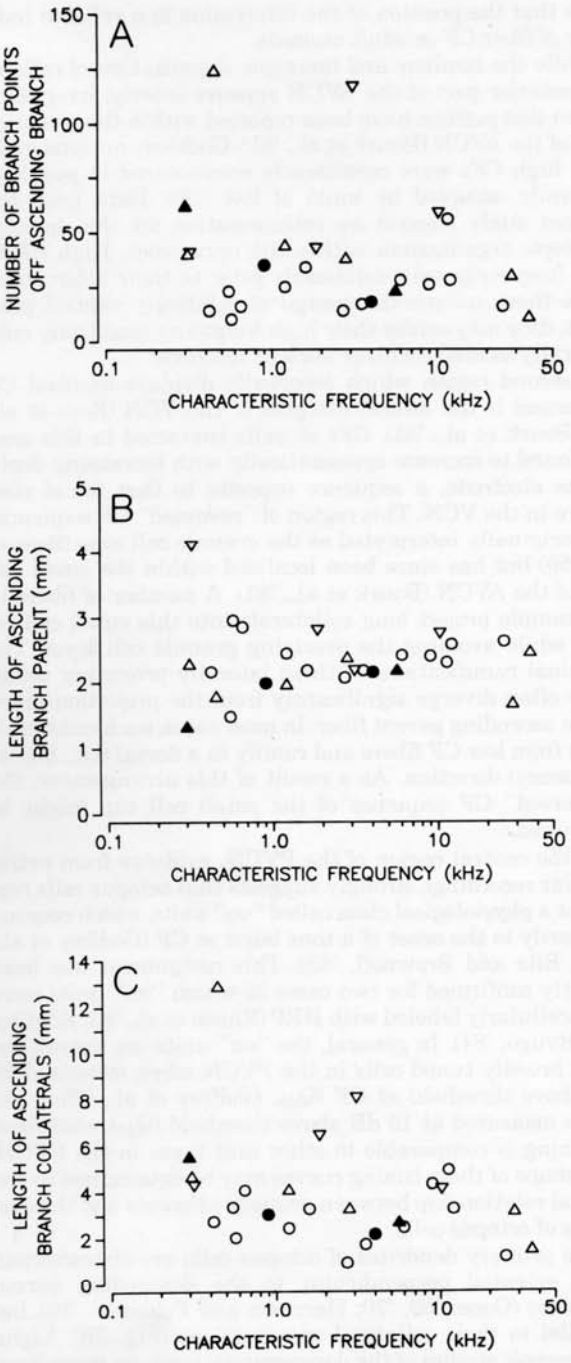

Fig. 16. Morphometry of the ascending branch. A. The number of branch points arising from the ascending branch. B. The length of the ascending branch parent axon. C. The total length of the collateral arborization arising from the ascending branch. Symbols are the same as in Figure 6.

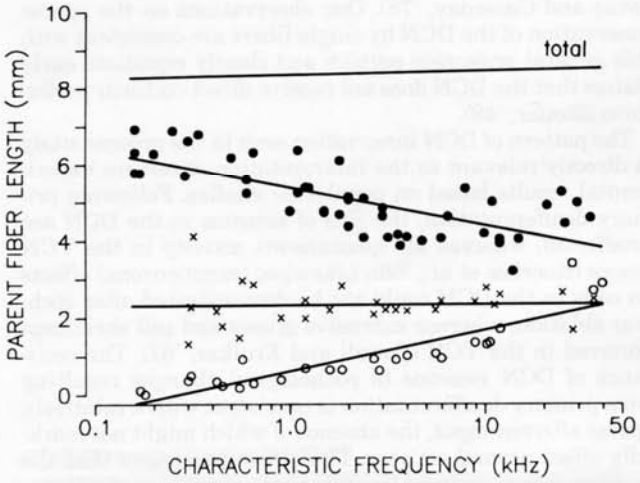

Fig. 17. Axon segment length for the central processes of type I spiral ganglion cells plotted as a function of CF. These measures were corrected for the depth of travel through each section by using the Pythagorean theorem. The lengths of the segment from the habenula to the Schwann-glial border (i.e., the intracochlear axon) are depicted by filled circles and were taken from a previous report (Liberman and Oliver, '84). Axon length from the Schwann-glial border to the bifurcation (i.e., the root branch) are indicated by open circles. The x's indicate axon length from the bifurcation to the anteriormost endbulb of Held (i.e., the ascending branch parent). Best-fit regression lines through the points are also shown. The top line is the sum of the three regression lines obtained from independent measures of the different axon segments and represents the "average" length of the central process from the organ of Corti to the anterior-most endbulb as a function of CF.

spiral ganglion neurons giving rise to the specific radial fibers (contacting inner hair cells), the spiral fibers (contacting outer hair cells), and the unspecific radial fibers (contacting a number of inner hair cells at considerable distances from each other).

Despite age differences between the cats in the present study and kittens used by Lorente de Nó, our fibers could be roughly grouped according to his classification scheme of ascending branches. When the resulting groups are examined with respect to their physiological response properties, however, no clear structure-function relationship is apparent. Furthermore, Lorente de Nó's speculation of the cochlear origin of these fiber groups is not supported, since all three types of central patterns have been observed following intracellular injection, a method which seems to label only type I spiral ganglion neurons contacting inner hair cells via specific radial fibers (Liberman, '82a,b; Liberman and Oliver, '84).

An interesting difference in the neonatal and adult morphology of the ascending branches is suggested by a comparison of Figures 3–9 and 3–10 (Lorente de Nó, '81) and Figures 5 and 15 in the present study (see also Fig. 1 of Ryugo and Fekete, '82). Such a comparison suggests that the ascending branches of mature cats emit a greater number of primary collaterals than those of kittens. These differences are probably not due to differences in techniques since HRP and Golgi methods yield the same images at comparable ages (Ryugo and Fekete, '82). Thus, it would appear that individual auditory nerve fibers sprout collaterals during postnatal maturation.

Primary afferent innervation of the DCN

Earlier studies using both silver-degeneration and autoradiographic methods have suggested a heavier cochlear projection to the VCN than to the DCN. Typically, the deep polymorphic layer of the DCN receives a moderate projection from the auditory nerve, while the deep portions of the fusiform cell layer receive only sparse projections (Stotler, '53; Powell and Cowan, '62; Osen, '70; Cohen et al., '72;

Jones and Casseday, '78). Our observations on the sparse innervation of the DCN by single fibers are consistent with this general projection pattern and clearly repudiate early claims that the DCN does not receive direct cochlear projections (Stotler, '49).

The pattern of DCN innervation seen in the present study is directly relevant to the interpretation of certain experimental results based on population studies. Following primary deafferentation, the SRs of neurons in the DCN are unaffected, whereas all spontaneous activity in the VCN ceases (Koerber et al., '66). Likewise, transneuronal effects on cells in the DCN could not be demonstrated after cochlear ablation, whereas extensive gliosis and cell shrinkage occurred in the VCN (Powell and Erulkar, '62). The resistance of DCN neurons to pathological changes resulting from primary deafferentation is consistent with a relatively sparse afferent input, the absence of which might not markedly affect normal activity. These results suggest that the auditory nerve may not be a predominant source of afferent input to the DCN.

The diameters of HRP-labeled type I axons and their collaterals within the DCN are relatively fine (generally less than 1 μm), in contrast to those described from Golgi studies (e.g., Lorente de Nó, '81). These observations may be relevant to the interpretation of degeneration results. If argyrophilic particle size is an accurate indicator of the caliber of degenerating axons and terminals, then one would expect primarily fine particulate debris in the DCN following degeneration of type I axons. It has been suggested that the presence of both coarse and fine argyrophilic debris in the chinchilla DCN following acoustic trauma represents differential degeneration of inner and outer hair cell systems (Morest and Bohne, '83). One link in their chain of arguments attributes coarse particulate debris to degeneration of type I neurons following the loss of inner hair cells and fine-to-moderate-sized debris to degeneration of type II neurons following the loss of outer hair cells. Barring major species differences, the small diameter of type I collaterals found in the DCN complicates interpretations which rely on differences in axon diameter to identify type I and type II fiber systems.

Characteristic frequency and tonotopic organization

Based on data from Golgi-stained material, early anatomists (Ramón y Cajal, '09; Poljak, '27; Lorente de Nó, '33) postulated that the laminar arrangement of primary afferent fibers to the cochlear nucleus reflected a cochleotopic pattern of projections. A correspondence was suggested between the position of the bifurcation and the longitudinal location of the spiral ganglion cell along the cochlear partition. The topographic projection of the cochlea onto the cochlear nucleus was grossly verified by experimentally mapping the pattern of degeneration following partial cochlear lesions in several different mammalian species (Sando, '65; Osen, '70; Webster, '71; Moskowitz and Liu, '72; Noda and Pirsig, '74). Basal parts of the cochlea, representing high frequencies, projected to dorsal regions of the cochlear nucleus, while apical, low-frequency portions of the cochlea projected to ventral regions. These anatomical results are consistent with the electrophysiological data reporting a tonotopic organization for the cochlear nucleus (Rose et al., '59; Evans and Nelson, '73; Goldberg and Brownell, '73; Kiang et al., '75; Bourk et al., '81). We have confirmed these earlier studies by directly demonstrating on a cell-by-cell basis that the position of the bifurcation is a reliable indicator of fiber CF in adult animals.

While the laminar and tonotopic organization of cells in the anterior part of the AVCN appears orderly, irregularities in this pattern have been reported within the posterior part of the AVCN (Bourk et al., '81). Cochlear nucleus units with high CFs were consistently encountered in positions generally occupied by units of low CFs. Data from the present study suggest an interpretation for the unusual tonotopic organization within the nerve root. High CF fibers frequently emit collaterals prior to their bifurcation. Since these collaterals emerge at relatively ventral positions, they may confer their high-frequency sensitivity onto ventrally located cochlear nucleus neurons.

A second region which reportedly displays unusual CF sequences is the lateral margins of the VCN (Rose et al., '59; Bourk et al., '81). CFs of units contacted in this area are found to increase systematically with increasing depth of the electrode, a sequence opposite to that found elsewhere in the VCN. This region of "reversed" CF sequences was originally interpreted as the granule cell area (Rose et al., '59) but has since been localized within the small cell cap of the AVCN (Bourk et al., '81). A number of fibers in our sample project long collaterals into this small cell region while avoiding the overlying granule cell layer. The terminal ramifications of these laterally projecting collaterals often diverge significantly from the projection plane of the ascending parent fiber. In most cases, such collaterals arise from low CF fibers and ramify in a dorsal (i.e., higher frequency) direction. As a result of this arrangement, the "reversed" CF sequence of the small cell cap might be explained.

In the central region of the PVCN, evidence from extracellular recordings strongly suggests that octopus cells represent a physiological class called "on" units, which respond primarily to the onset of a tone burst at CF (Godfrey et al., '75a; Ritz and Brownell, '82). This assignment has been directly confirmed for two cases in which "on" units were intracellularly labeled with HRP (Rhode et al., '83; Rouiller and Ryugo, '84). In general, the "on" units are among the most broadly tuned cells in the PVCN when measured 20 dB above threshold at CF (Q_{20}, Godfrey et al., '75a). Yet when measured at 10 dB above threshold (Q_{10}), sharpness of tuning is comparable to other unit types in the PVCN. The shape of these tuning curves may be determined by the spatial relationship between primary afferents and the dendrites of octopus cells.

The primary dendrites of octopus cells are characteristically oriented perpendicular to the descending parent branches (Osen, '69, '70; Harrison and Feldman, '70), but parallel to their collateral ramifications (Fig. 5B). Light-microscopic studies of the degenerating auditory nerve have demonstrated preterminal argyrophilia associated with the dendrites of octopus cells (Kane, '73). This parallel alignment of dendrites and collateral ramifications may provide the anatomical basis for both the sharpness of frequency selectivity near threshold and the broad tuning at higher intensities. Certain spatial relationships would permit a maximal number of synaptic contacts to be made between a few fibers of similar CFs and the dendrites of a particular octopus cell. Such primary input could be expected to dominate the octopus cell response at low stimulus levels, perhaps accounting for the sharp tuning near threshold. Due to spatial constraints, however, individual fibers having higher or lower CFs would make relatively fewer synaptic

contacts with that particular octopus cell; consequently, at low stimulus levels, their respective inputs would not be sufficient to activate the cell. At high stimulus levels, more primary fibers representing a wider range in frequencies would be activated. This summed activity from many fibers converging onto individual octopus cells might account for the broader frequency response (compared to other cochlear nucleus neurons or auditory nerve fibers).

Within this central region, primary collaterals and their ramifications cascade down from the parent axons of the descending branches. This anatomical arrangement suggests that a tonotopic map of the octopus cells, obtained by recording from cell bodies, would be spatially offset relative to that of primary fibers. Thus, the CFs of octopus cells should be higher than those of the immediately surrounding parent fibers. Finally, since the octopus cell region does not appear to receive innervation from all fibers of very low CFs, low frequencies might be poorly represented by the octopus cell. Although "on" units are not plentiful in the frequency range below 1 kHz (Godfrey et al., '75a; Ritz and Brownell, '82), the data might also reflect a sampling bias in the recording procedure.

Morphological correlates of spontaneous rate

SR differences among labeled auditory nerve fibers are closely correlated with morphological differences in the caliber and location of the peripheral termination on the body of the inner hair cell (Liberman, '82a). The unmyelinated terminal portions of high SR fibers typically have larger diameters than low or medium SR fibers. There is also a spatial separation of terminals around the inner hair cell according to SR. The terminal swellings of high SR fibers are found on the side of the inner hair cell closest to the outer hair cells, whereas the terminal swellings of low and medium SR fibers are found on the side nearest the modiolus. We have determined that these peripheral differences are correlated with differences in the central projections.

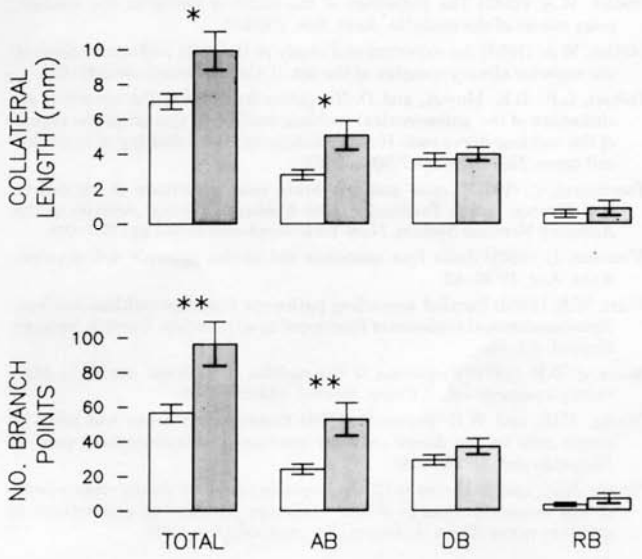

Fig. 18. Histograms of the mean collateral lengths and numbers of branch points for high SR fibers (open bars) compared to low and medium SR fibers (shaded bars). Brackets indicate the standard error of the mean. Abbreviations: AB, ascending branch; DB, descending branch; RB, root branch. Symbols: (*) $p < .02$, (**) $p < .01$, using Student's t-test.

The ascending branches of low and medium SR fibers have more complex ramifications and wider spatial distributions in the AVCN than those of high SR fibers (Fig. 18).

On the basis of regional differences in SR-related branching patterns, we can now focus our investigations on the nature of these particular specializations. Since the outputs of the cochlear nucleus are organized according to specific cell types (Harrison and Feldman, '70; Ryugo et al., '81; Cant, '82; Tolbert et al., '82; Adams, '83), and since different pathways may be specialized for certain auditory functions (e.g., pathway for sound localization, middle ear muscle reflexes, or pattern discrimination), it is important to establish whether different cell types receive different patterns of auditory nerve input. A functional segregation of ascending auditory pathways may already be established by the pattern of primary input to the cochlear nucleus.

ACKNOWLEDGMENTS

The authors wish to thank Dr. Nelson Kiang for his support and helpful suggestions in the preparation of the manuscript. We gratefully acknowledge the assistance of Rebecca Cronin Schreiber in most phases of the work. Technical contributions were also made by Leslie Dodds, Peter Ley, Patricia McGaffigan, Barbara Norris, Mary Oliver, Guy Pugh, and Kathleen Wallace. Finally, thanks are due to Robert Brown, Mark Curby, Ishmael Stefanov-Wagner, and David Steffens of the Eaton-Peabody Laboratory engineering staff. This work was supported by NIH grants NS 13126 and NS 18339. D.M.F. was supported by an NSF predoctoral fellowship and by a Ryan Foundation fellowship (Cincinnati, Ohio). E.M.R. was supported by the Swiss Foundation for Fellowships in Medicine and Biology (Basel, Switzerland). Portions of these results were presented in preliminary form at the 96th meeting of the American Association of Anatomists, Atlanta, Georgia, 1983.

LITERATURE CITED

Adams, J.C. (1983) Multipolar cells in the ventral cochlear nucleus project to the dorsal cochlear nucleus and the inferior colliculus. Neurosci. Lett. *37*:205–208.

Arnesen, A.R., and K.K. Osen (1978) The cochlear nerve in the cat: Topography, cochleotopy, and fiber spectrum. J. Comp. Neurol. *178*:661–678.

Bourk, T.R., J.P. Mielcarz, and B.E. Norris (1981) Tonotopic organization of the anteroventral cochlear nucleus of the cat. Hearing Res. *4*:215–241.

Brawer, J.R., and D.K. Morest (1975) Relations between auditory nerve endings and cell types in the cat's anteroventral cochlear nucleus seen with the Golgi method and Nomarski optics. J.Comp. Neurol. *160*:491–506.

Brawer, J.R., D.K. Morest, and E.C. Kane (1974) The neuronal architecture of the cochlear nucleus of the cat. J. Comp. Neurol. *155*:251–300.

Cant, N.B. (1982) Identification of cell types in the anteroventral cochlear nucleus that project to the inferior colliculus. Neurosci. Lett. *32*:241–246.

Cant, N.B., and D.K. Morest (1978) Axons from non-cochlear sources in the anteroventral cochlear nucleus of the cat. A study with the rapid Golgi method. Neuroscience *3*:1003–1029.

Cohen, E.C., J.R. Brawer, and D.K. Morest (1972) Projections of the cochlea to the dorsal cochlear nucleus in the cat. Exp. Neurol. *35*:450–479.

Evans, E.F., and P.G. Nelson (1973) The responses of single neurons in the cochlear nucleus of the cat as a function of their location and the anaesthetic state. Exp. Brain Res. *17*:402–427.

Evans, E.F., and A.R. Palmer (1980) Relationship between the dynamic range of cochlear nerve fibers and their spontaneous activity. Exp. Brain Res. *40*:115–118.

Feldman, M.L., and J.M. Harrison (1969) The projection of the acoustic nerve to the ventral cochlear nucleus of the rat. A Golgi study. J. Comp. Neurol. *137*:267–294.

Frank, E., W.A. Harris, and M.B. Kennedy (1980) Lysophosphatidyl choline facilitates labeling of CNS projections with horseradish peroxidase. J. Neurosci. Methods *2*:183–189.

Godfrey, D.A., N.Y.-S. Kiang, and B.E. Norris (1975a) Single unit activity in the posteroventral cochlear nucleus of the cat. J. Comp. Neurol. *162:*247–268.

Godfrey, D.A., N.Y.-S. Kiang, and B.E. Norris (1975b) Single unit activity in the dorsal cochlear nucleus of the cat. J. Comp. Neurol. *162:*269–284.

Goldberg, J.M., and W.E. Brownell (1973) Discharge characteristics of neurons in anteroventral and dorsal cochlear nuclei of cat. Brain Res. *64:*35–54.

Harrison, J.M., and M.L. Feldman (1970) Anatomical aspects of the cochlear nucleus and superior olivary complex. Contrib. Sensory Physiol. *4:*95–142.

Held, H. (1983) Die centrale Gehörleitung. Arch. Anat. Physiol. *17:*201–248.

Jones, D.R., and J.H. Casseday (1978) Auditory nerve: Projections from cochlea demonstrated by autoradiographic methods. Brain Res. *148:*224–229.

Kane, E.C. (1973) Octopus cells in the cochlear nucleus of the cat: Heterotypic synapses upon homeotypic neurons. Int. J. Neurosci. *5:*251–279.

Kiang, N.Y.-S. (1975) Stimulus representation in the discharge pattern of auditory neurons. In D.B. Tower (ed): The Nervous System, Vol. 3, Human Communication and its Disorders. New York: Raven Press, pp. 81–96.

Kiang, N.Y.-S., D.A. Godfrey, B.E. Norris, and S.E. Moxon (1975) A block model of the cat cochlear nucleus. J. Comp. Neurol. *162:*221–246.

Kiang, N.Y.-S., J.M. Rho, C.C. Northrup, M.C. Liberman, and D.K. Ryugo (1982) Hair-cell innervation by spiral ganglion cells in adult cats. Science *217:*175–177.

Kiang, N.Y.-S., T. Watanabe, E.C. Thomas, and L.F. Clark (1965) Discharge Patterns of Single Fibers in the Cat's Auditory Nerve. Cambridge: MIT Press.

Kim, D.O., and C.E. Molnar (1979) A population study of cochlear nerve fibers: Comparison of spatial distributions of average-rate and phase-locking measures of responses to single tones. J. Neurophysiol. *42:*16–30.

Koerber, K.C., R.R. Pfeiffer, W.B. Warr, and N.Y.-S. Kiang (1966) Spontaneous spike discharges from single units in the cochlear nucleus after destruction of the cochlea. Exp. Neurol. *16:*119–130.

Kölliker, A. (1896) Hanbuch der Gewebelehre des Menschen, 6 Aufl., Bd. 2, S.799. Leipzig: Engelmann.

Liberman, M.C. (1978) Auditory-nerve response from cats raised in a low-noise chamber. J. Acoust. Soc. Am. *63:*442–455.

Liberman, M.C. (1982a) Single-neuron labelling in the cat auditory nerve. Science *216:*1239–1241.

Liberman, M.C. (1982b) The cochlear frequency map for the cat: Labelling auditory-nerve fibers of known characteristic frequency. J. Acoust. Soc. Am. *72:*1441–1449.

Liberman, M.C., and M.E. Oliver (1984) Morphometry of intracellularly labelled neurons of the auditory-nerve: Correlations with functional properties. J. Comp. Neurol. *223:*163–176.

Lorente de Nó, R. (1933) Anatomy of the eighth nerve. The central projection of the nerve endings of the internal ear. Laryngoscope *43:*1–38.

Lorente de Nó, R. (1981) The Primary Acoustic Nuclei. New York: Raven Press.

Morest, D.K. (1968) The growth of synaptic endings in the mammalian brain: A study of the calyces of the trapezoid body. Z. Anat. Entwicklungsgesch. *127:*201–220.

Morest, D.K., and B.A. Bohne (1983) Noise-induced degeneration in the brain and representation of inner and outer hair cells. Hearing Res. *9:*145–151.

Moskowitz, N., and J-C. Liu (1972) Central projections of the spiral ganglion of the squirrel monkey. J. Comp. Neurol. *144:*335–344.

Mugnaini, E., W.B. Warr, and K.K. Osen (1980) Distribution and light microscopic features of granule cells in the cochlear nucleus of cat, rat, and mouse. J. Comp. Neurol. *191:*581–606.

Noda, Y., and W. Pirsig (1974) Anatomical projection of the cochlea to the cochlear nuclei of the guinea pig. Arch. Otorhinolaryngol. *208:*107–120.

Osen, K.K. (1969) Cytoarchitecture of the cochlear nuclei in the cat. J. Comp. Neurol. *136:*453–484.

Osen, K.K. (1970) Course and termination of the primary afferents in the cochlear nuclei of the cat: an experimental anatomical study. Arch. Ital. Biol. *108:*21–51.

Peters, A., S.L. Palay, and H.deF. Webster (1976) The Fine Structure of the Nervous System: The Neurons and Supporting Cells. Philadelphia: W.B. Saunders Co.

Pfeiffer, R.R. (1966) Classification of response patterns of spike discharges for units in the cochlear nucleus: tone burst stimulation. Exp. Brain Res. *1:*220–235.

Poljak, S. (1927) Über den allgemeinen Bauplan des Gehörsystems und über seine Bedeutung für die Physiologie, für die Klinik und für die Psychologie. Z. Gesamte Neurol. Psychiatr. *110:*1–49.

Powell, T.P.S., and W.M. Cowan (1962) An experimental study of the projection of the cochlea. J. Anat. *96:*269–284.

Powell, T.P.S., and Erulkar (1962) Transneuronal cell degeneration in the auditory relay nuclei of the cat. J. Anat. *96:*249–268.

Ramón y Cajal, S. (1909) Histologie du Système Nerveux de l'Homme et des Vertébrés, Vol. I. Madrid: Instituto Ramón y Cajal (1952 reprint), pp. 754–838.

Rhode, W.S., and D. Oertel, and P.H. Smith (1983) Physiological response properties of cells labeled intracellularly with horseradish peroxidase in cat ventral cochlear nucleus. J. Comp. Neurol. *213:*448–463.

Ritz, L.A., and W.E. Brownell (1982) Single unit analysis of the posteroventral cochlear nucleus of the decerebrate cat. Neuroscience *7:*1995–2010.

Rose, J.E., R. Galambos, and J.R. Hughes (1959) Microelectrode studies of the cochlear nuclei of the cat. Bull. Johns Hopkins Hospital *104:*211–251.

Rouiller, E.M., and D.K. Ryugo (1984) Intracellular marking of physiologically characterized neurons in the ventral cochlear nucleus of the cat. J. Comp. Neurol. *225:*167–186.

Ryugo, D.K., and D.M. Fekete (1982) Morphology of primary axosomatic endings in the anteroventral cochlear nucleus of the cat: A study of the endbulbs of Held. J. Comp. Neurol. *210:*239–257.

Ryugo, D.K., F.H. Willard, and D.M. Fekete (1981) Differential afferent projections to the inferior colliculus from the cochlear nucleus in the albino mouse. Brain Res. *210:*342–349.

Sachs, M.B., and P.J. Abbas (1974) Rate versus level functions for auditory-nerve fibers in cats: tone-burst stimulation. J. Acoust. Soc. Am. *56:*1835–1847.

Sachs, M.B., and E.D. Young (1979) Encoding of steady-state vowels in the auditory nerve: Representation in terms of discharge rate. J. Acoust. Soc. Am. *66:*470–480.

Sando, I. (1965) The anatomical interrelationships of the cochlear nerve fibers. Acta Otolaryngol. *59:*417–436.

Schalk, T.B., and M.B. Sachs (1980) Nonlinearities in auditory-nerve fiber responses to bandlimited noise. J. Acoust. Soc. Am.*67:*903–913.

Spoendlin, H. (1969) Innervation patterns in the organ of Corti of the cat. Acta Otolaryngol. *67:*239–254.

Stotler, W.A. (1949) The projection of the cochlear nerve on the acoustic relay nuclei of the medulla. Anat. Rec. *103:*561.

Stotler, W.A. (1953) An experimental study of the cells and connections of the superior olivary complex of the cat. J. Comp. Neurol. *98:*401–423.

Tolbert, L.P.. D.K. Morest, and D. Yurgelun-Todd (1982) The neuronal architecture of the anteroventral cochlear nucleus of the cat in the region of the cochlear nerve root: Horseradish peroxidase labelling of identified cell types. Neuroscience 7:3031–3052.

Tsuchitani, C. (1978) Lower auditory brain stem structures of the cat. In R.F. Newton and L. Fernandez (eds): Evoked Electrical Activity in the Auditory Nervous System. New York: Academic Press, pp. 373–401.

Vincenzi, L. (1901) Sulla fina anatomia del nucleo ventrale dell'acustico. Anat. Anz. *19:*33–42.

Warr, W.B. (1982) Parallel ascending pathways from the cochlear nucleus: Neuroanatomical evidence of functional specialization. Contrib. Sensory Physiol. *7:*1–38.

Webster, D.B. (1971) Projection of the cochlea to cochlear nuclei in Merriam's kangaroo rat. J. Comp. Neurol. *143:*323–340.

Young, E.D., and W.E. Brownell (1976) Responses to tones and noise of single cells in the dorsal cochlear nucleus of unanesthetized cats. J. Neurophysiol. *39:*282–300.

Young, E.D., and M.B. Sachs (1979) Representation of steady-state vowels in the temporal aspects of the discharge patterns of populations of auditory-nerve fibers. J. Acoust. Soc. Am. *66:*1381–1403.